Geometric Analysis of Intracoronary Pressure Curves

Marta Gonçalves Alves

marta.g.alves@tecnico.ulisboa.pt

Instituto Superior Técnico, Universidade de Lisboa

October 2019

Abstract

Coronary physiology assessment tests are used to evaluate the physiological severity of angiographically intermediate coronary stenotic lesions. iFR and cFFR are indicators, used in clinical practice, that quantify the ratio between the pressure distal and proximal to a stenosis in predefined zones of the pressure recordings. In this thesis, it is proposed that the severity of a coronary lesion can be related with the geometry of the pressure curve distal to the stenosis. In order to test this hypothesis, a software was developed where pressure recordings were analysed and five new geometric indices were automatically computed in different zones of the cardiac cycle. The commercially available indices, obtained from the device used in clinical practice, were compared to the same emulated indices computed by this new software. The correlation coefficients obtained ($r^2 > 0.97$) in these comparisons suggest a correct automatic identification of cycles and curve time points, validating the method for their automatic detection. The validation of the new physiological indices was performed by comparing them to the iFR, considering a reduced dataset of 39 runs. The indicator that presented the most significant correlation with iFR was Index 7 ($y = 0.77x - 0.506$; $r^2 = 0.2$). These results suggest that the geometrical behaviour of the distal pressure curve is correlated with the severity of coronary lesions, as evaluated with established indices. This finding may have clinical applicability, which should be evaluated in a clinical prospective study.

Keywords: Coronary Physiology; Pressure curve geometry; Instantaneous wave-free ratio; Contrast induced hyperaemia

1. Introduction

Due to ageing of the population and its sedentary life habits, mainly in the western world, hypertension, hyperglycemia and excess of adipose tissue are becoming more common in today's population. CAD (Coronary Artery Disease) is one of the pathologies that results from the interaction of these risk factors with blood cells and blood vessels walls and is characterized by the accumulation of atherosclerotic plaque in coronary arteries [1]. This disease plays an important role in today's society once it affects a great part of the population, being the leading cause of death worldwide [2].

In order to suit the decision on whether to treat or not and to choose the most appropriate treatment method to apply in each case, it is crucial to have a diagnosis tool that could provide reliable information on the severity of each lesion. Therefore, several diagnosis tools are available in clinical practice, from non-invasive to invasive techniques as is the case of coronary angiography [3, 4].

In most part of the cases, coronary angiography is used to determine the severity of each lesion. However, this method only provides a visual estimation of the lumen diameter reduction of the damaged vessel, not giving information on the functional consequences of each lesion. Thus, angiographically intermediate lesions are often submitted to physiological assessment tests that provide a measurement of the functional significance of the lesion [5].

The gold-standard method for physiological lesion assessment is FFR (Fractional Flow Reserve) [6, 7]. However, the administration of adenosine to induce maximal hyperaemia, needful to measure FFR, can cause side effects [8]. Therefore, some alternatives to FFR have been proposed as is the case of the iFR (Instantaneous Wave-Free Ratio) [9]. iFR is measured at rest avoiding the need of hyperaemia and, subsequently, the administration of adenosine. However, this indicator is commercially restricted to a single software proprietary which limits its extended clinical application. The fact that the contrast agent normally used in clinical practice could induce submaximal hyperaemia,

led to the development of an indicator, similar to FFR, that makes use of contrast medium instead of adenosine to induce hyperaemia, the cFFR (Contrast Fractional Flow Reserve) [10, 11]. There are many limitations to the use of cFFR, such as the absence of a dedicated software, the need to record a damped proximal pressure due to contrast injection and the lack of an established protocol for data acquisition. The main goal of this work is to implement a computational algorithm to compute a shape based indicator, using only the distal pressure, able to classify lesion significance from pressure curves under contrast hyperaemia.

2. Methods

2.1. Data acquisition

The dataset analysed in this work was acquired by the multidisciplinary team (cardiologists, cardiopneumology and radiology technicians and nursing staff) of the Digital Angiography and Interventional Cardiology Unit, the catheterization laboratory (cath lab) of Hospital do Espírito Santo - Évora (HESE). In the HESE cath lab, there are two different sets of hardware and software available, developed by two different companies, that collect intracoronary pressure recordings and measure the severity of stenoses present in coronary arteries. These machines are the Quantien™ console from Abbott compatible with the PressureWire™ X pressure guide wire and the CORE™ console from Philips that uses the Volcano Verrata® Plus pressure guide wire to measure intracoronary pressure.

Lesions with 50 to 70% of lumen diameter reduction are considered as angiographically intermediate. In this case, angiogram does not give clear information on the severity of the lesion and, subsequently, its impact on myocardial perfusion. Therefore, when clinically indicated, patients presenting lesions within this range of severity were submitted to a physiology assessment test in order to clarify whether that lesion would benefit from a revascularization helping the cardiologist in that decision.

From 2015 to 2019, 122 patients with intermediate angiographic lesions were submitted to a physiological severity assessment. The dataset obtained from these medical exams forms a total of 769 runs - 324 iFR runs, 88 RFR runs, 42 FFR runs and 179 cFFR runs (the remaining 136 were excluded from analysis).

2.2. Data Processing

Once the files were exported from the proprietor hardware, data were analysed using Python™(Python Software Foundation, https://www.python.org/). The data processing initiates with importation of the files exported from the proprietary software to Python. After the importation, distal (Pd) and aortic (Pa) pressure recordings are filtered using regularization method 1.

2.3. Run Identification

Once the filtering is achieved, the identification of each run is required given that each run type present different characteristic features.

The input files included three types of runs - iFR, FFR and cFFR (RFR runs where classified as iFR runs). Each of these run types has specific characteristics that enables is classification.

iFR runs were identified as lasting less than 15 seconds. Runs lasting more than 15 seconds and that exhibited an injection artifact - artifact caused by the intracoronary injection of a contrast medium - were considered to be cFFR runs. Runs longer than 1 minute were identified as FFR runs. Lastly, runs that did not fit any of the above mentioned parameters were classified as unidentified.

Previously to run identification, some runs were excluded from analysis once they were not relevant to this work. Examples of these runs are: pullback runs, drift check runs and error runs.

2.4. Definition of Zones

In order to study the pressure recordings and extract information about the relationship between its geometrical behaviour and the severity of the lesion in question, zones of interest, useful to the calculation of new indices, were defined (Figure 1).

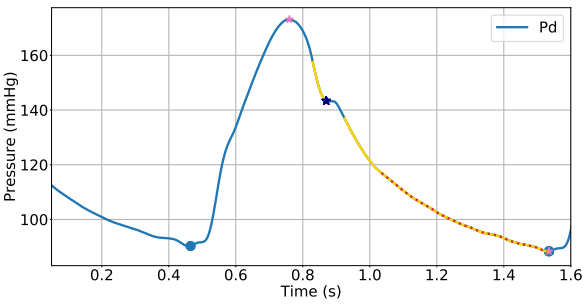

Figure 1: Different zones defined in the a cardiac cycle. Beginning and end of the cardiac cycle (**blue** circle). Dicrotic notch (**dark blue** star). Wave-free period (dashed line in **red**). Period 2 and period 3 (**yellow** line). Beginning and end of Period 1 (**pink** star.) Distal pressure curve in **blue**. Pressure in mmHg and time in seconds.

Cardiac Cycle The beginning of each cardiac cycle was defined as the zero of the Geometric measure C of the pressure curve between the minimum of the previous cycle and the maximum of the cycle in question. For this, a mean value for the length of a cycle in a specific run was estimated and the search for the onset of the cycle was restricted to this estimated period. The end of each cardiac cycle matches the beginning of the previous cycle.

Dicrotic Notch Based on previous works from different authors [12, 13], a dicrotic notch detection algorithm was developed. First of all, for each cycle, three geometric measures, A, B and C, were defined. Geometric measure C was used to compute the dicrotic notch. In cases where the waveform exhibited an incisura rather than a defined dicrotic notch, this point is not present. In these situations, the incisura was defined using geometric measure A.

Wave-Free Period For each cycle, the diastole was defined as the period between the dicrotic notch and the beginning of the following cycle discarding the small oscillations that could occur in the final 30% of the cycle. Therefore, the beginning of the WFP (Wave-Free Period) was identified as the point 25% after the beginning of the diastole and its end coincident to the end of the diastole.

Other Zones Additionally to the delineation of the WFP, other zones of interest were defined with the aim of studying the geometrical behaviour of the intracoronary pressure curves during these periods. Period 1, period 2 and period 3 were then defined accordingly to Figure 1.

2.5. Resting and hyperaemia detection

Regarding cFFR runs, it is crucial to delimit two time intervals - the resting period and the hyperaemic period. The resting period is the period before the intracoronary injection of contrast medium that would induce hyperaemia and the hyperaemic period is this time interval where the coronaries are under the effect of this hyperaemic agent. The injection of contrast medium in the coronaries causes an abruptly change in aortic pressure, here called injection artifact. This injection artifact was identified as the zone where aortic pressure is below 40 Hgmm. Figure 2 exhibits resting, hyperaemic and injection zones in a cFFR run.

The resting zone was defined as the zone between the beginning of the pressure recording and the beginning of the injection zone. Within this zone, there were delimited the three resting cycles that corresponded to the three cycles presenting more stability, meaning that the mean difference between their consecutive peaks was minimum. These peaks location was obtained using the Python function *find_peaks* from the signal processing toolbox.

The hyperaemic zone was identified as the zone starting four cycles from the end of the injection zone and ending twenty from the end of the injection zone. The three hyperaemic cycles are the three consecutive cycles, within the hyperaemic zone, which presented the maximum hyperaemia, in other words, the maximal difference between mean aortic pressure and mean distal pressure.

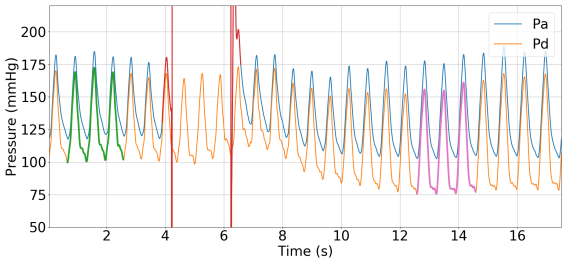

Figure 2: Identification of resting, hyperaemic and injection zones. Distal pressure curve (Pd) in blue. Aortic pressure curve (Pa) in orange. Resting cycles in **green**. Hyperaemic cycles in pink. Injection artifact in red. Pressure expressed in mmHg and time expressed in seconds.

2.6. Computation of indices

Subsequently to the identification of the different zones and points of interest in the pressure curves, several indices were computed with the aim of obtaining a correlation between these indices and the indices normally used in clinical practice - iFR and cFFR.

Commonly Used Indicators iFR was computed, accordingly to its definition [9], as the mean ratio between the mean distal pressure and the mean aortic pressure both computed during the WFP. RFR was calculated, accordingly to its definition [14], as the lowest ration between distal and aortic pressure measurements calculated as a moving average. For this moving average it was considered a 9 points moving average. cFFR was computed, accordingly to FFR definition [6], as the ratio between the mean distal pressure and the mean aortic pressure computed during hyperaemia induced by contrast medium, choosing the three more hyperaemic cycles.

Index 1 With the hypothesis that the area between aortic and distal pressure curves could have a good correlation with iFR, an index that could measure this feature was computed. This is what we call index 1. Therefore, index 1 aims to differentiate between the two cases in Figure 3.

Index 2 Visual observation of the geometric shape of distal pressure curves, taken from our dataset, led to the formulation of the following hypothesis: Is increasing stenotic severity correlated with increasingly steepest pressure decrease?

In order to test this hypothesis, index 2 was computed.

Index 3 A simpler method to verify the hypothesis of steepest pressure decrease, in the case of more

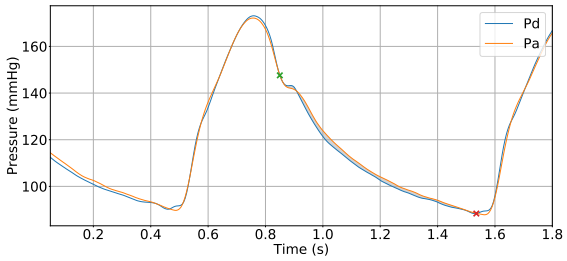

Figure 3: Identification of the area between aortic and distal pressure curves between t_a and t_b. Distal pressure curve (Pd) in blue. Aortic pressure curve (Pa) in orange. Area between Pd and Pa curves in grey. t_a in green. t_b in red. Pressure expressed in mmHg and time expressed in seconds.

severe stenosis was also considered. It consists of Index 3, computed as a ratio during period 1.

It was hypothesised that in the negative cases, i.e. non-significant lesions, index 3 should be closer to one.

Index 4 By visual analysis of several iFR runs, it was hypothesised that the maximum of geometric measure B on the period 3 would reflect a concavity, analogous to the curve ventricularization seen in significant lesions, and hence have a correlation with iFR value.

Therefore, this index was computed using the geometric measure B during period 3.

Indices 5 and 6 As mentioned above, the geometric shape of a pressure curve can be understood through the geometric measures B and C. In an attempt to find possible relations between these measures, with both iFR and cFFR, several indices were analysed, at different moments of the cardiac cycle.

Therefore, the mean distal and aortic pressure geometric measures during each of the zones delimited in the cardiac cycle, mentioned above, were computed. Subsequently, the values on Period 2 and 3 were compared. This was performed in order to detect the differences of pressure along the stenosis.

Regularization Method 2 Despite the application of the regularization method 1, as mentioned above, some small oscillations still persist in the filtered pressure curves. Such oscillations propagate in the computations, therefore affecting the results.

With the aim of eliminating this small oscillations, Periods 2 and 3 of each cardiac cycle of the distal and aortic pressure curves were regularized using what we called method 3.

Indices 3, 5 and 6 were then computed now using the regularized zones.

2.7. Statistical Analysis

The relationship between indices was quantified by the application of a linear regression and subsequent determination of the correlation coefficient, r^2. The diagnostic accuracy of the test was measured, using the ROC (Receiver Operating Characteristic) curve, by the calculation of the AUC (Area Under the Curve). This statistical method enabled the identification of each index optimal cutoff corresponding to iFR and RFR ≤ 0.89 or cFFR ≤ 0.83. The performance of each index in predicting a positive iFR, RFR or cFFR was assessed by PPV (Positive Predictive Value), NPV (Negative Predictive Value), sensitivity and specificity using the cutoff chosen. The optimal cutoff was computed as the point where the Youden's Index was maximal [15].

3. Results

3.1. Validation of the Software

Instantaneous Wave-Free Ratio The iFR values obtained from Philips machine and the results obtained for iFR using this new software were compared. The analysis of Figure 4, depicting the linear correlation line from the relation between both iFR values (from the software available in HESE and the new software developed), shows a very significant correlation between these two indices with $r^2 = 0.991$.

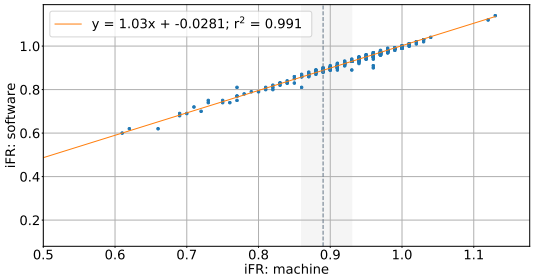

Figure 4: Linear correlation between iFR values computed by the software used in clinical practice in HESE and the ones calculated using the software developed in this work. Dashed line indicates the cutoff value of 0.89 (in grey) for iFR considered in clinical practice. Light grey shaded area represents iFR grey zone (0.86-0.93).

Resting Full-Cycle Ratio The software from Abbott makes use of a resting index different from iFR, the RFR. Therefore, the same analysis was performed as for iFR correlating the RFR values computed by the machine at HESE and the RFR values calculated using the present software. The linear regression analysis, depicted in Figure 5, shows a correlation with $r^2 = 0.973$ and a line equation of $y = 1.07x - 0.0819$ suggesting a good correlation between the two measurements.

Contrast Fractional Flow Reserve The determination of the hyperaemic cycles considered into the calculation of cFFR frequently represents a challenge for the software available in clinical practice. Therefore, the software often fails on the lo-

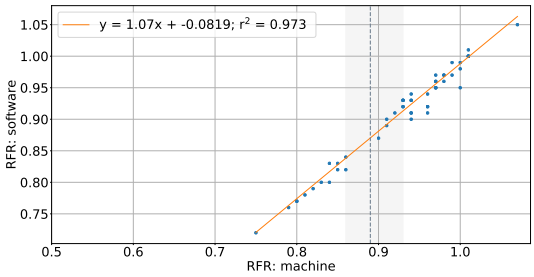

Figure 5: Linear correlation between RFR values computed by the software used in clinical practice in HESE and the ones calculated using the software developed in this work. Dashed line indicates the cutoff value of 0.89 (in grey) for RFR considered in clinical practice. Light grey shaded area represents iFR grey zone (0.86-0.93).

cation of these cycles due to the existence of the injection artifact that may induce the software to error. The cFFR values are then frequently deviated from the correct values and need the revision from a cardiologist that detects the error and selects, manually, the location where the cFFR should have been computed.

The cFFR values computed by the software developed in this work were then compared to cFFR values from the manual measurements using the software available at HESE. The linear correlation between these two quantities ($y = 0.967x + 0.0364$; $r^2 = 0.993$) is exhibited in Figure 6.

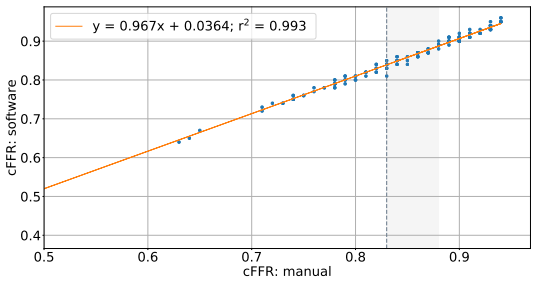

Figure 6: Linear correlation between cFFR values computed by the software used in clinical practice in HESE and the ones calculated using the software developed in this work. Linear regression with correlation coefficient of 0.993 and line equation $y = 0.967x + 0.0364$. Dashed line indicates the cutoff value of 0.89 (in grey) for cFFR considered in clinical practice. Light grey shaded area represents iFR grey zone (0.86-0.93).

3.2. Instantaneous Wave-Free Ratio Runs

The dataset selected to this analysis excludes runs where either the detection of the dicrotic notch (4 runs) or the delineation of the cycles (17 runs) presented any kind of error due to artifacts such as extrasystoles or atrial fibrillation. Runs where, despite the good detection of the different zones in the curve, distal pressure was bigger than aortic pressure (18 runs), atrial fibrillation (21 runs), extrasystoles (3 runs) or other type of artifact (21 runs) were present, were also excluded from this analysis. A prior analysis on the influence of hypotension on curve geometry led to the exclusion of runs (48 runs) from patients presenting hypotension, i.e. patients where the systolic pressure was below 110 mmHg. Therefore, a total of 278 iFR runs were considered in this analysis.

Index 1 The relation between the indicator that measures Index 1 and iFR, considering all runs of the dataset, is depicted in Figure 7a. As expected, a very significant correlation ($y = -0.779 + 0.785$; $r^2 = 0.979$) was obtained between these two indices.

Additionally, an AUC of the ROC curve of 0.99 was obtained, corroborating the hypothesis that this indicator has a very high diagnosis accuracy when using iFR as the reference gold-standard method. From this analysis, a cutoff value of 0.0853 was computed corresponding to a PPV of 88.4% and a NPV of 99.0% with a sensitivity of 97.4% and a specificity of 95.3%.

Index 2 The comparison between Index 2 and the iFR values, considering the complete dataset available, is exhibited in Figure 7b. Despite presenting a pour correlation ($y = -0.516x + 0.627$; $r^2 = 0.271$), it is still possible to denote a tendency in Figure 7b where lower values correspond to higher iFR values and, consequently, less significant stenoses. On the other hand, larger areas do not seem to be closely associated with iFR value. In fact, considering a cutoff value of 0.13, obtained through the ROC curve analysis, a NPV of 91.4% was obtained, corroborating that observation. Additionally, the PPV was 42.9%. These values correspond to a sensitivity and a specificity of 84.6% and 59.1%, respectively.

Index 7 A comparison between Index 7 and the iFR was obtained and is presented in Figure 7c. From this comparison, a poor correlation was obtained between the two indicators ($y = 0.77x - 0.506$; $r^2 = 0.2$). In spite of this observation, a moderate tendency could be denoted in Figure 7c where higher Index 7 values seem to correspond to higher values of iFR, although the opposite is not verified.

Supporting these observations, considering a cutoff value of 0.14, computed using the ROC curve, a NPV of 87.3% and a PPV of 58.4% were obtained with a sensitivity of 66.7% and a specificity of 82.8%.

Index 4 Considering Index 4, the relationship between this index and iFR is plotted in Figure 7d. A low correlation coefficient was obtained ($y = -7079.0x + 9610.0$; $r^2 = 0.189$) indicating a very weak relation between the Index 4 and iFR.

Additionally, a PPV and a NPV of 41.5% and 87.4% were obtained, respectively with a sensitivity of 75.6% and a specificity of 61.4%, considering a cutoff value of 2860.

Index 6 Despite presenting a significant diagnostic accuracy (AUC of the ROC curve of 0.82), the correlation obtained between Index 6 and the iFR value was very weak ($y = -0.796x + 0.802$; $r^2 = 0.0493$). This correlation is depicted in Figure 7e. Considering a cutoff value corresponding to a Index 6 of 0.0547, computed as the maximal Youden Index, a PPV of 60.5% and a NPV of 87.4% were obtained with corresponding sensitivity of 66.7% and a specificity of 84.2%.

3.3. Index 7 as an Indicator of Curve Geometry

Concerning the correlations obtained, a moderate tendency seems to exist for the Index 7. The relation obtained between the Index 7 and iFR suggests that higher Index 7 correspond to higher iFR values. Thus, this index will be used in the next sections as an example of an indicator of the curve geometry.

3.4. Index 8

Using Index 7 for both distal and aortic pressure curves, Index 8 was also computed and compared to iFR. This index was computed in an attempt to normalize Index 7 computed in the distal pressure curve and, consequently, get a curve geometry indicator that would have a better correlation with iFR than the ones previously presented in this work.

A good correlation, depicted in Figure 8a was verified between this indicator and iFR ($y = 2.46x - 1.6$; $r^2 = 0.42$). A tendency where higher Index 7 values correspond to higher iFR values and *vice versa* is also suggested.

An analysis of the ROC curve, exhibited in Figure 8b, shows a good diagnostic accuracy of this indicator in predicting iFR (AUC = 0.84). A cutoff value of 0.649, a PPV of 56.1% and a NPV of 93.0% were obtained with corresponding sensitivity and specificity of 85.7% and 73.7%, respectively.

3.5. Contrast Induced Hyperaemia Runs

After selecting the distal pressure Index 7, measured in the Period 1 of the curve, as the indicator that presents the more significant relation with iFR, an analysis comparing this indicator with cFFR was performed.

The dataset considered in these analyses excluded runs presenting artifacts such as extrasystoles (5 runs), atrial fibrillation (4 runs) and other artifacts (2 runs), runs with errors in the detection of the cycles (6 runs), in the detection of the dicrotic notch (7 runs) and in the detection of hyperaemic (1 run) or resting regions (2 runs) and runs where the systolic pressure at rest was below 110 mmHg (23 runs).

Distal Pressure Index 7 In order to verify the relation existent between distal pressure Index 7 and cFFR, comparisons were obtained for the distal pressure Index 7 measured in the cycles under contrast induced hyperaemia (Figure 9a).

Despite the moderate correlation ($y = 0.604x - 0.412$; $r^2 = 0.205$) obtained, a tendency can be observed where higher Index 7 values correspond to higher cFFR values. Furthermore, the ROC curve analysis (Figure 9b) performed for the distal pressure Index 7 measured at hyperaemia, considering cFFR as the reference gold-standard method, revealed a good diagnosis accuracy (AUC = 0.81). From this analysis, considering a cutoff value of 0.07, a PPV of 74.4% and a NPV of 76.5% with a sensitivity and a specificity of 62.7% and 84.9%, respectively.

Index 8 On the other hand, in order to test the relation between the Index 8 and cFFR, the linear correlation between these two indices was also obtained for the hyperaemic cycles. These results are presented Figure 9c. A significant correlation was obtained ($y = 2.32x$ 1.57; $r^2 = 0.395$) and are coherent with the ones obtained in the previous section (Figure 8a) to the comparison with iFR.

Additionally, the ROC curve analysis (Figure 9d) performed suggested that this index present a significant diagnosis accuracy when considering cFFR as the reference gold standard method. Namely, an AUC of the ROC curve of 0.81 was obtained. Moreover, considering a cutoff of 0.357, a PPV of 69.0% and a NPV of 83.3% were computed, with a sensitivity and a specificity of 78.4% and 75.3%, respectively.

4. Discussion

4.1. Validation of the Software

Instantaneous Wave-Free Ratio The small variations to the linear regression line exhibited in Figure 4 may be explained by small differences in the calculus of the location of the dicrotic notch along with variations in the detection of the end of the WFP that are not explicit in the work of Sen *et al.* [9]. Despite that, the strong correlation obtained validates the methodology followed in the computation of the iFR index.

Resting Full-Cycle Ratio The small deviations to the RFR values obtained in the catheterization laboratory present in Figure 5 are caused by variations in the calculation of this index. This index is computed as the lowest ratio between distal and aortic pressures during an entire cycle calculated as a moving average. Thus, differences in the number of points considered for the calculation of this moving average will cause variations in the measures.

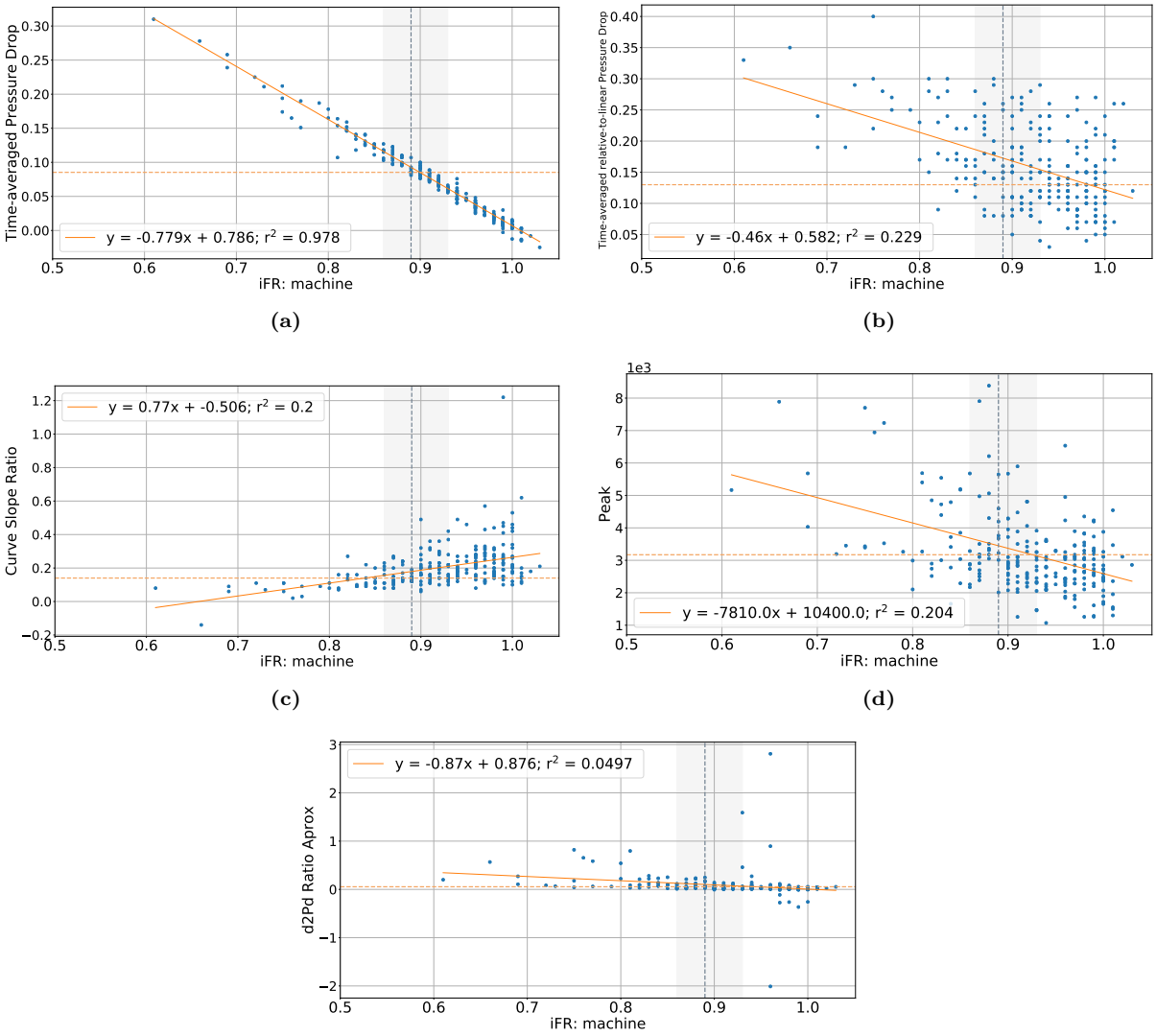

Figure 7: Linear regression correlating new indices to iFR. Dashed line in grey indicating the cutoff value considered for iFR (0.89). Light grey shaded area representing iFR grey zone (0.86-0.93). Dashed line in orange indicating the cutoff value computed for the referred index through ROC curve. **(a)** Index 1 (cutoff = 0.0853); **(b)** Index 2 (cutoff = 0.13); **(c)** Index 7 (cutoff = 0.14); **(d)** Index 4 (cutoff = 3170); **(e)** Index 6 (cutoff = 0.0547).

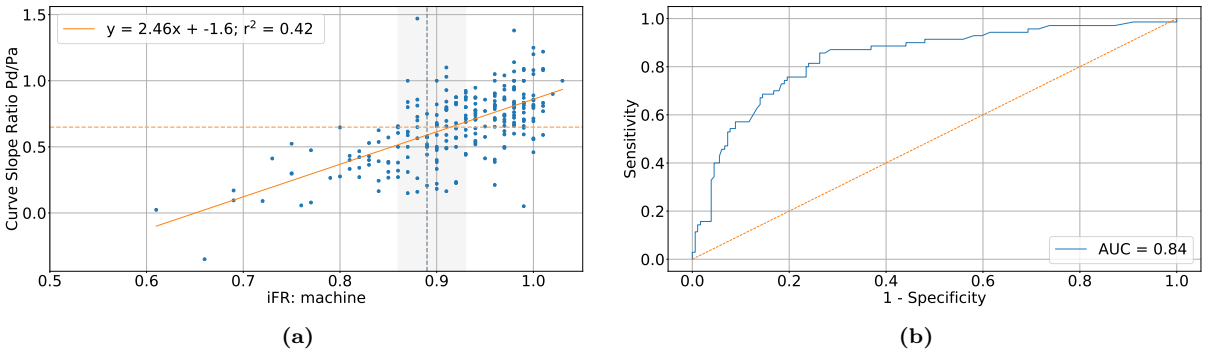

Figure 8: **(a)** Linear regression correlating Index 7 to iFR value. Dashed line in grey indicating the cutoff value considered for iFR (0.89). Light grey shaded area representing iFR grey zone (0.86-0.93). Dashed line in orange indicating the cutoff value computed for the referred index through ROC curve (0.15). **(b)** ROC curve (in blue) for the area between line and distal pressure curve using iFR as the reference gold-standard variable with a threshold cutoff of 0.89.

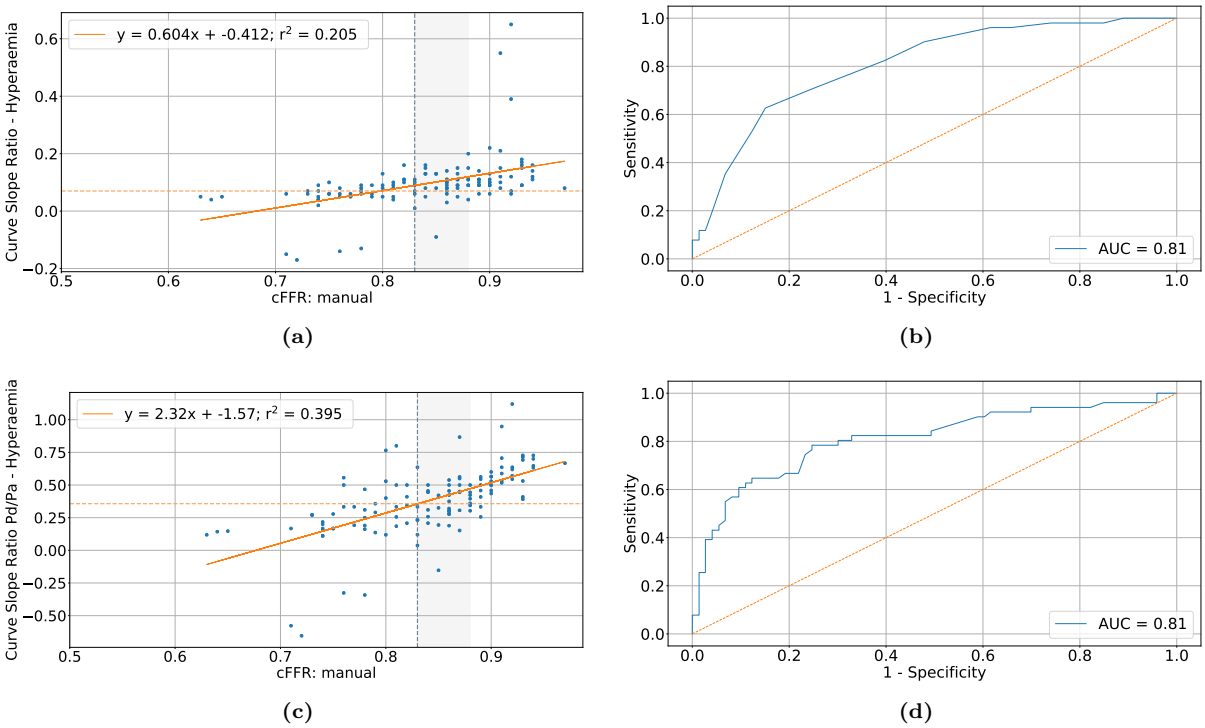

Figure 9: Linear regressions (left) and ROC curve (right) correlating Index 7 on distal pressure (top) and Index 8 (bottom) to cFFR value. Dashed line in grey indicating the cutoff value considered for cFFR (0.83). Light grey shaded area representing iFR grey zone (0.83-0.98). Dashed line in orange indicating the cutoff value computed for the referred index.

Contrast Fractional Flow Reserve The slight oscillations existing in this correlation could be explained by the way this index is computed by the machine and confirmed by a cardiologist. In the commercial software, cFFR is computed as a moving average of the ratio between distal and aortic pressure in the more hyperaemic point, where the difference between distal and aortic pressure is maximal. On the other hand, in this work cFFR is computed as an average of the three more hyperaemic cycles making the measurements potentially less prone to suffer rapid variations and, consequently, be more robust.

4.2. Instantaneous Wave-Free Ratio Runs

The Index 1 seems to be a very good predictor of the severity of a lesion, being closely correlated with iFR. However, some limitations on the use of iFR also persist when using this index. This is the case of issues such as errors in the equalization of the two pressure sensors, aortic and distal. Thus, other indices that consider only the distal pressure curve will be analysed, despite their lower correlation with iFR.

Despite the pour correlations obtained for the Index 2, Index 7 and the Index 4, a tendency seems to be present on these relations. For the Index 2 and for the Index 4, lower values appear to correspond to higher iFR values and, consequently, to less significant lesions. In fact, the correlations obtained in an analysis where only 39 runs were considered, revealed better correlations ($r^2 = 0.577$ for Index 2; $r^2 = 0.572$ for the Index 7; $r^2 = 0.393$ for the Index 4) where this tendency was clear.

Index 8 These results suggest that this indicator, that is based on the geometry of the curve, provides a reasonable alternative to iFR. Additionally, cases where the pressure sensors are not equalized would benefit from this index once it only depends on the shape of the pressure curve and not on the pressure values.

4.3. Summary

Firstly, regarding iFR runs, despite presenting moderate to low correlation coefficients, indices as the Index 2 and the Index 7 show a tendency with iFR. While higher Index 2 values appear to be associated with lower iFR values, higher Index 7 values seem to be related to higher iFR values. Therefore, distal pressure curve of more significant stenosis seems to decrease and reach lower values faster after systolic peak than less significant stenosis. These results could suggest that the Index 7 permitted to capture the difference in slopes existing between Periods 2 and 3 of the distal pressure curve and the Index 2, allowed a quantification of the concavity of the Period 1 of the distal pressure curve.

On the other hand, indices as the Index 4 and the Index 6 showed a poor correlation and no tendency.

This poor correlation, could be explained by the existence of several outliers in the dataset that influence the correlations. Thus, it is expected that a more rigorous analysis of the dataset, with patient-level fine tuning of the algorithm and eliminating other runs that may have quality anomalies, could lead to a better correlations between these indices and iFR.

5. Conclusions

In this work, several aspects regarding coronary stenosis evaluation with pressure wires were concluded. Firstly, this work have suggested that it seems possible to measure lesion severity (estimate lesion severity as assessed by conventional indices) by analysing pressure curve shape, regardless of its absolute value. Secondly, this evaluation could be done by analysing the distal pressure only. Finally, it is possible to automate contrast-induced hyperaemia determination in a robust way.

Acknowledgement

This document was written and made publicly available as an institutional academic requirement and as a part of the evaluation of the MSc thesis in Biomedical Engineering of the author at Instituto Superior Técnico. The work described herein was performed at the Department of Mathematics of Instituto Superior Técnico (Lisbon, Portugal) and at Digital Angiography and Interventional Cardiology Unit of the cardiology department of Hospital do Espírito Santo - Évora under the CORE project (University of Évora, HESE), during the period February-October 2019, under the supervision of Prof. Jorge Tiago, Dr. David Neves and Prof. Lino Patrício.

References

[1] Libby P. and Theroux P., "Pathophysiology of Coronary Artery Disease The Pathophysiology of Chronic CAD," *Circulation*, vol. 111, pp. 3481–3488, 2005.

[2] "Global Health Estimates 2016: Deaths by Cause, Age, Sex, by Country and by Region, 2000-2016," 2018.

[3] Roffi M., Patrono C., Collet J. P., Mueller C., Valgimigli M., Andreotti F., Bax J. J., Borger M. A., Brotons C., Chew D. P., Gencer B., Hasenfuss G., Kjeldsen K., Lancellotti P., Landmesser U., Mehilli J., Mukherjee D., Storey R. F., Windecker S., Baumgartner H., Gaemperli O., Achenbach S., Agewall S., Badimon L., Baigent C., Bueno H., Bugiardini R., Carerj S., Casselman F., Cuisset T., Erol Ç., Fitzsimons D., Halle M., Hamm C., Hildick-Smith D., Huber K., Iliodromitis E., James S., Lewis B. S., Lip G. Y., Piepoli M. F., Richter D., Rosemann T., Sechtem U., Steg P. G., Vrints C., and Zamorano J. L., "2015 ESC Guidelines for the management of acute coronary syndromes in patients presenting without persistent st-segment elevation: Task force for the management of acute coronary syndromes in patients presenting without persistent ST-segment elevation of ," *European Heart Journal*, vol. 37, no. 3, pp. 267–315, 2016.

[4] Bresnahan J. F., "Textbook of Interventional Cardiology," *Mayo Clinic Proceedings*, vol. 70, no. 7, p. 719, 1995.

[5] Shah S. and Pfau S., "Coronary Physiology in the Cardiac Catheterization Laboratory," *Journal of Clinical Medicine*, vol. 8, no. 2, p. 255, 2019.

[6] Pijls N. H., Van Son J. A., Kirkeeide R. L., De Bruyne B., and Gould K. L., "Experimental basis of determining maximum coronary, myocardial, and collateral blood flow by pressure measurements for assessing functional stenosis severity before and after percutaneous transluminal coronary angioplasty," *Circulation*, vol. 87, no. 4, pp. 1354–1367, 1993.

[7] Knuuti J., Wijns W., Saraste A., Barbato E., Capodanno D., Funck-brentano C., Prescott E., Storey R. F., Deaton C., Cuisset T., Agewall S., Dickstein K., Edvardsen T., Escaned J., Gersh B. J., Svitil P., Gilard M., Hasdai D., Hatala R., Mahfoud F., Masip J., Muneretto C., Valgimigli M., Achenbach S., and Bax J. J., "2019 ESC Guidelines for the diagnosis and management of chronic coronary syndromes The Task Force for the diagnosis and management of chronic," *European Heart Journal*, pp. 1–71, 2019.

[8] Lee J. Z., Singh N., Nyotowidjojo I., Howe C., Low S. W., Nguyen T., Pinto D., Kumar G., and Lee K. S., "Comparison of regadenoson and nitroprusside to adenosine for measurement of fractional flow reserve: A systematic review and meta-analysis," *Cardiovascular Revascularization Medicine*, vol. 19, no. 2, pp. 168–174, 2018.

[9] Sen S., Escaned J., Malik I. S., Mikhail G. W., Foale R. A., Mila R., Tarkin J., Petraco R., Broyd C., Jabbour R., Sethi A., Baker C. S., Bellamy M., Al-Bustami M., Hackett D., Khan M., Lefroy D., Parker K. H., Hughes A. D., Francis D. P., Di Mario C., Mayet J., and Davies J. E., "Development and validation of a new adenosine-independent index of stenosis severity from coronary waveintensity analysis: Results of the ADVISE (ADenosine Vasodilator Independent Stenosis Evaluation) study," *Journal of the American College of Cardiology*, vol. 59, pp. 1392–1402, apr 2012.

[10] Guzman S. V. and West J. W., "Cardiac effects of intracoronary arterial injections of various roentgenographic contrast media," *American Heart Journal*, vol. 58, no. 4, pp. 597–607, 1959.

[11] Leone A. M., Scalone G., De Maria G. L., Tagliaferro F., Gardi A., Clemente F., Basile E., Cialdella P., De Caterina A. R., Porto I., Aurigemma C., Burzotta F., Niccoli G., Trani C., Rebuzzi A. G., and Crea F., "Efficacy of contrast medium induced Pd/Pa ratio in predicting functional significance of intermediate coronary artery stenosis assessed by fractional flow reserve: Insights from the RINASCI study," *EuroIntervention*, vol. 11, no. 4, pp. 421–427, 2015.

[12] Li B. N., Dong M. C., and Vai M. I., "On an automatic delineator for arterial blood pressure waveforms," *Biomedical Signal Processing and Control*, vol. 5, no. 1, pp. 76–81, 2010.

[13] Oppenheim M. J. and Sittig D. F., "An innovative dicrotic notch detection algorithm which combinesrule-based logic with digital signal processing techniques," *Computers and Biomedical Research*, vol. 28, no. 2, pp. 154–170, 1995.

[14] Svanerud J., Ahn J. M., Jeremias A., Van 'T Veer M., Gore A., Maehara A., Crowley A., Pijls N. H., De Bruyne B., Johnson N. P., Hennigan B., Watkins S., Berry C., Oldroyd K. G., Park S. J., and Ali Z. A., "Validation of a novel non-hyperaemic index of coronary

artery stenosis severity: The Resting Full-cycle Ratio (VALIDATE RFR) study," *EuroIntervention*, vol. 14, no. 7, pp. 806–814, 2018.

[15] Habibzadeh F., Habibzadeh P., and Yadollahie M., "On determining the most appropriate test cut-off value: The case of tests with continuous results," *Biochemia Medica*, vol. 26, no. 3, pp. 297–307, 2016.